Nanotechnology **18** (2007) 135102 (8pp) doi:10.1088/0957-4484/18/13/135102

In situ observation of fluoride-ion-induced hydroxyapatite–collagen detachment on bone fracture surfaces by atomic force microscopy

J H Kindt[1,4], P J Thurner[2,4,5], M E Lauer[2], B L Bosma[3], G Schitter[2], G E Fantner[2], M Izumi[3], J C Weaver[3], D E Morse[3] and P K Hansma[2]

[1] Veeco Metrology Inc., 112 Robin Hill Road, Goleta, CA 93117, USA
[2] Physics Department, University of California Santa Barbara, Santa Barbara, CA 93106, USA
[3] Department of Molecular, Cellular and Developmental Biology, University of California Santa Barbara, Santa Barbara, CA 93106, USA

E-mail: thurner@physics.ucsb.edu

Received 17 November 2006, in final form 10 January 2007
Published 28 February 2007
Online at stacks.iop.org/Nano/18/135102

Abstract
The topography of freshly fractured bovine and human bone surfaces was determined by the use of atomic force microscopy (AFM). Fracture surfaces from both kinds of samples exhibited complex landscapes formed by hydroxyapatite mineral platelets with lateral dimensions ranging from ∼90 nm × 60 nm to ∼20 nm × 20 nm. Novel AFM techniques were used to study these fracture surfaces during various chemical treatments. Significant topographical changes were observed following exposure to aqueous solutions of ethylenediaminetetraacetic acid (EDTA) or highly concentrated sodium fluoride (NaF). Both treatments resulted in the apparent loss of the hydroxyapatite mineral platelets on a timescale of a few seconds. Collagen fibrils situated beneath the overlying mineral platelets were clearly exposed and could be resolved with high spatial resolution in the acquired AFM images. Time-dependent mass loss experiments revealed that the applied agents (NaF or EDTA) had very different resulting effects. Despite the fact that the two treatments exhibited nearly identical results following examination by AFM, bulk bone samples treated with EDTA exhibited a ∼70% mass loss after 72 h, whereas for the NaF-treated samples, the mass loss was only of the order of ∼10%. These results support those obtained from previous mechanical testing experiments, suggesting that enhanced formation of superficial fluoroapatite dramatically weakens the protein–hydroxyapatite interfaces. Additionally, we discovered that treatment with aqueous solutions of NaF resulted in the effective extraction of noncollagenous proteins from bone powder.

(Some figures in this article are in colour only in the electronic version)

1. Introduction

Bone, as well as other natural materials such as wood, sponge skeletons and mollusk shells, exhibits a complex structure with several hierarchical levels ranging from the macro-down to the nanoscale [1–8]. All of these hierarchical levels of complexity influence the mechanical behaviour of bone. However, as argued by Gao *et al*, the nanostructural aspect of bone makes it a material that becomes insensitive to random flaws at the molecular level such that material performance in terms of fracture toughness is optimized [9]. At the nanostructural

[4] These authors contributed equally to this work.
[5] Author to whom any correspondence should be addressed.

level, bone consists of (A) collagen type I molecules that assemble first into microfibrils [10], which in turn assemble into fibrils with typical average diameters of ∼90 nm [1], (B) platelet-shaped mineral crystals of hydroxyapatite (calcium phosphate; $Ca_5(PO)_4(OH)$) with typical average dimensions of ∼50 nm × 25 nm × 3 nm [3, 11, 12], (C) water and (D) several noncollagenous proteins (NCPs) [13]. It is generally accepted that collagen fibrils, mineral platelets and water are important for the mechanical properties of bone, whereas this role has only recently been suggested for the NCPs [14]. However, the general importance of the organic–inorganic interface for the mechanical properties in bone was already proposed in the earlier work of Walsh *et al* [15, 16].

Despite the fact that the NCPs make up only a few per cent by mass of the bone material, they might very well have a profound effect on fracture toughness, in a similar manner as was observed in connection with the organic matrix of abalone nacre [17]. It was also found recently that the majority of plastic deformation of compact bone in tension does not occur within the collagen fibrils, but elsewhere in the material [18]. In addition, there exists experimental evidence that bone fails by delamination [19, 20] in the interfibrillar space, i.e. by the separation of mineralized collagen fibrils [14, 21, 22], and that the amount and composition of the NCPs changes with age and disease [13]. As previously studied by mechanical testing and ultrasound velocity measurements, NaF deteriorates bone mechanical properties, which has been ascribed to a weakening of the organic–mineral interfacial bonding [16, 23–28]. Changes in the bones of animals fed a fluoride-rich diet have also been reported; slight increases in width and thickness of hydroxyapatite crystals and detrimental changes in bone mechanical properties were observed [29, 30]. However, the precise effect of NaF on bone ultrastructure is a matter of ongoing discussion and no direct observation of the hypothesized mineral–organic de-bonding exists to date.

To address this issue, we used high resolution atomic force microscopy (AFM), in conjunction with other techniques. AFM is a well-suited tool for the imaging of bone ultrastructure [31] as it provides nanometre spatial resolution without the need for extensive or potentially destructive sample preparation. This enables *in situ* imaging experiments, even in a hydrated environment, if necessary. For the investigation of bone and other biological nano-composite materials such as dentin, AFM can be used in combination with chemical agents to alter the investigated structure, i.e. dissolution of specific ultrastructural components or influencing the interface of two or more components. Thus, this approach allows a direct investigation of the changes in bone ultrastructure following treatment with a variety of chemical or biochemical agents. The insights gained can then be used to explain and interpret results obtained from other macroscopic experiments, such as mechanical testing, on similarly treated samples, in an ultrastructural context. Using such a chemical approach, which was previously also applied by Habelitz *et al* [32] to study dentin, we investigated the effect of NaF and EDTA on trabecular bone fracture surfaces *in situ* and in a time-lapsed fashion. Whereas EDTA is known to chelate Ca^{2+} ions in solution, leading to the dissolution of hydroxyapatite crystals [33], NaF was previously inferred to influence their interfacial bonding to the organic components of bone [16].

2. Materials and methods

2.1. Sample preparation

Trabecular regions of bovine or human vertebrae were cut into cuboids measuring ∼4 mm × 4 mm × 5 mm under constant irrigation using a bone bandsaw (Marmed Inc., Cleveland, OH, USA), and the marrow was removed with a water jet (Waterpik Technologies, Fort Collins, CO, USA). For fracture surface investigations, the surfaces of the bone cuboids were stained with Coomassie Blue R-250 (Sigma-Aldrich, 0.2 g ml^{-1}) in Na-buffer (150 mM NaCl, 10 mM Hepes, pH 7.0) for 5 min, and then rinsed in Ca-buffer (110 mM NaCl, 40 mM $CaCl_2$, 10 mM Hepes, pH 7.0) to remove any excess stain. Subsequently, a stained bone cuboid was clamped in a vice, with the bone load axis parallel to the vice grip edge. The half of the cuboid extending from this vice was clamped into a second one. The cuboid was then pulled apart, i.e. fractured in tension. The two pieces were immediately rinsed briefly in HPLC grade water (EMD Chemicals Inc., Gibbstown, NJ, USA), blotted dry on a Kimwipe from the side not exposed by fracturing, and separately placed in centrifuge tubes with a small wad of Kimwipe at the bottom. The pieces were centrifuged for 5 min to remove any residual buffer and avoid artefacts from salt residues and desiccated in vacuum for at least 30 min. All these steps were designed to prevent modifications of the fracture surface after the fracture event, in particular the formation of salt crystals from residual buffer. To locate an area suitable for AFM imaging, the dried cube was placed under a dissection microscope. The Coomassie stain allowed us to clearly distinguish between stained external surfaces (blue) and unstained fracture surfaces (white). For AFM imaging, it is important to choose a sample surface that is reasonably smooth. Fracture areas, which appeared translucent underneath a dissecting microscope, turned out to be the most suitable for AFM investigation. Once identified, a trabecula with a promising fracture surface was removed with a scalpel, and glued onto a custom-made AFM sample disc, with a well in the centre, using epoxy resin (2-Ton Clear Epoxy, Devcon, Danvers, MA, USA) in such a manner that the surface to be investigated faced upward and was oriented roughly parallel to the sample disc.

2.2. AFM imaging

Samples were set up in an AFM (Multimode-Nanoscope IV, Veeco Inc., Santa Barbara, CA, USA) equipped with an E-scanner (Veeco Inc.) and a video microscope. Cantilevers were mounted in all cases in a multimode glass liquid cell [34, 35] fitted with an S-shaped silicone O-ring (Veeco Inc.). AFM imaging of human trabecular bone was done in Na-buffer, in contact mode, using a coated microlever (Model # MLCT-AUHW, Veeco Inc.) at a scan rate of 2 Hz. For imaging of bovine fractured surfaces, a silicon, tapping in air (Model # RTESPW, Veeco Inc.), cantilever was used. A dry N_2 gas source was furnished from a Dewar filled with liquid nitrogen, a 20 Ω, 25 W power resistor and a Variac variable transformer (Staco Energy Products Co., Dayton, OH, USA). The Dewar was connected to the liquid cell via several metres of tubing to allow the gas to equilibrate to room temperature before entering the fluid cell. The voltage was set to 7 V AC during

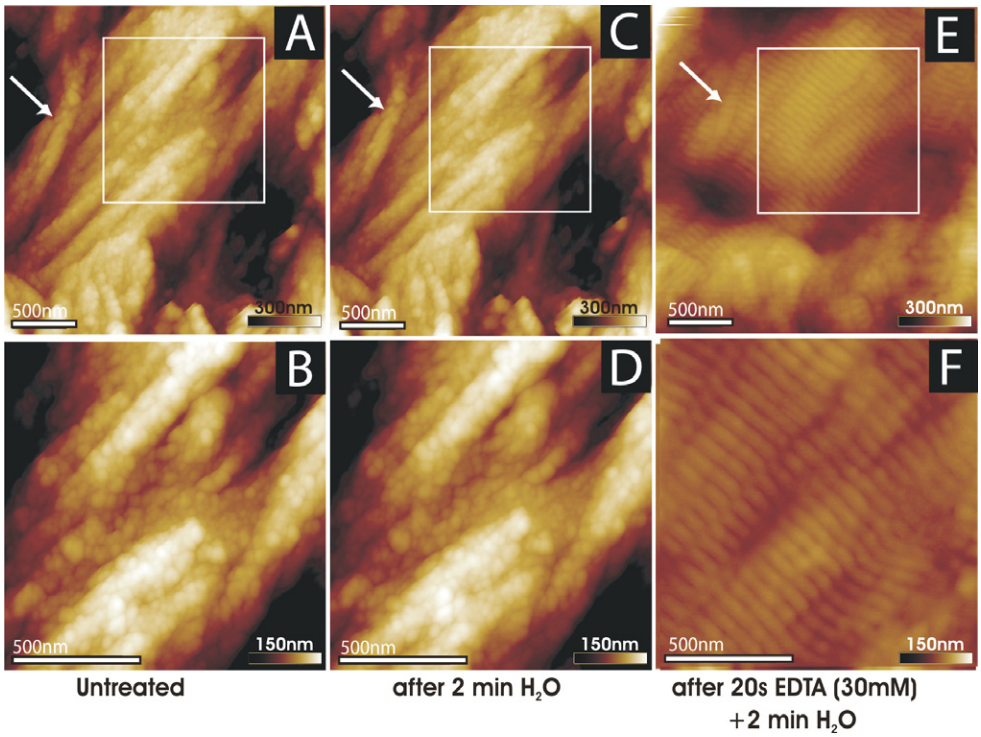

Figure 1. AFM height images of a fracture surface of bovine trabecular bone, imaged in N_2 gas, reveal collagen fibrils (A) densely coated with rounded mineral platelets (B) (close-up from (A), white frame). The surface remains unchanged after a 2 min H_2O rinse (C and D), but EDTA treatment for 10 s, followed by a 2 min H_2O rinse, removes the mineral platelets to reveal banded collagen fibrils at the same sample location (E) and (F). The same sample area was imaged before and after treatment, the white arrows point to the same reference fibril, oriented at an acute angle relative to the neighbouring fibrils, in each image.

imaging. The use of dry N_2 gas during AFM imaging was done in order to remove the hydration layer on the sample surface, which can degrade spatial resolution. Imaging was done in tapping mode and dry N_2 gas at a scan rate of 1 Hz.

2.3. Chemical sample treatment

2.3.1. Water control. The fluid cell was disconnected from the gas source and connected to a fluid source: a 60 ml syringe without plunger, filled with 60 ml of HPLC grade water. The syringe was raised above the level of the fluid cell (gravity feed [35]) to create a flow rate of about 0.5 ml s^{-1} inside the fluid cell. Subsequently, the liquid cell was reconnected to the dry gas source and the resistor voltage was set to 15 V AC for 20 min to dry the sample.

2.3.2. EDTA treatment. The fluid cell was disconnected from the gas source and 300 μl of 30 mM EDTA in a 10 mM Hepes, 150 mM NaCl buffer at pH 8.0, were slowly injected into the fluid cell. After 20 s, the sample was rinsed with 60 ml of HPLC grade water as described above. The liquid cell was then reconnected to the dry gas source and the resistor voltage set to 15 V AC for 20 min to dry the sample.

The cantilever resonance sometimes changed by an order of ∼0.1%, during treatment, probably because of residues eluded by the treatment adsorbed onto the cantilever, thus changing its mass slightly.

2.3.3. NaF treatment. Following the same procedure as for the EDTA treatment, 300 μl of saturated (∼1 M) NaF solution in 10 mM Hepes, 150 mM NaCl buffer at pH 7.0, were injected into the fluid cell and replaced with HPLC grade water after exposure times of 1 s. This short exposure time was achieved by injecting the 300 μl of NaF solution into a piece of tubing connected to the fluid cell. The other end of the tubing was then connected to a water reservoir; an open syringe containing 60 ml of HPLC grade water, mounted above the level of the fluid cell (gravity feed). Driven by the water, the NaF solution flowed through the AFM fluid cell (with a volume of 40 μl) in approximately 1 s and was then immediately washed out by the 60 ml of water.

A total of 12 samples were treated either with EDTA or NaF. The images shown in figures 1 and 2 show typical results obtained from these treatments.

2.4. Image processing

All presented AFM images are height data and images within each figure are on the same height scale. Unsharp masking (Photoshop, Adobe Systems Inc., San Jose, CA, USA) was used to improve small-feature visibility. Average particle sizes and standard deviations were determined from figures 1(B) and 2(B) by measuring length and width of 20 particles each. Both particle sizes and height profiles shown in figures 1 and 2 were determined using Nanoscope software (Veeco Inc.).

2.5. Mass comparison

For the time-resolved mass comparison, six bovine vertebral trabecular bone samples were used. These bone samples were

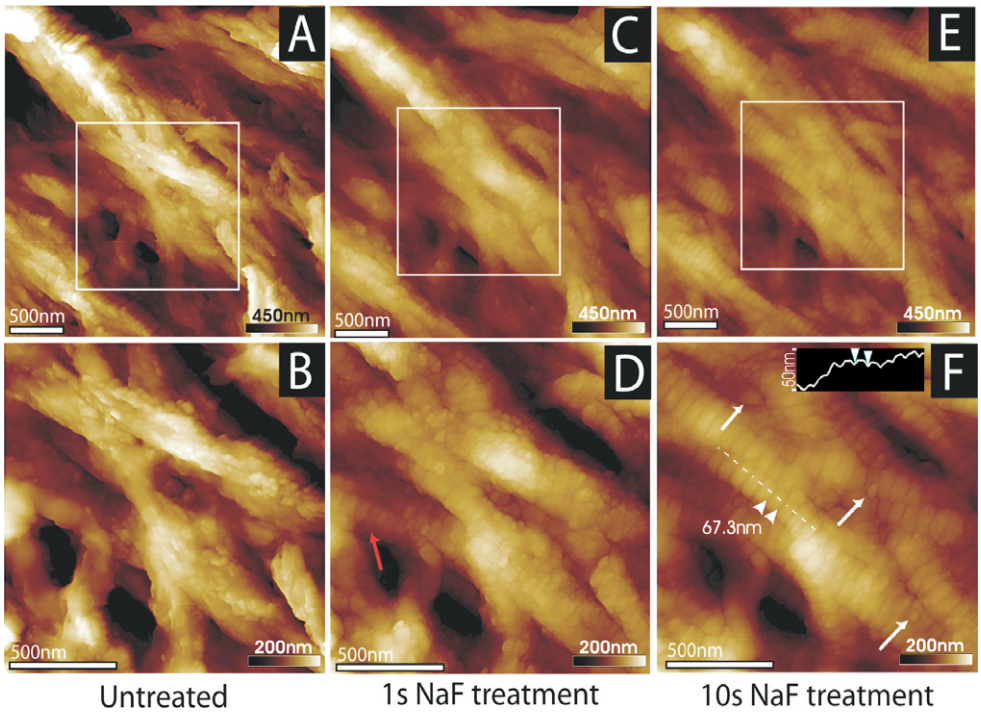

Figure 2. Time-resolved sequence of AFM images of a bovine trabecular bone fracture surface, imaged in N_2 gas, following NaF treatment show collagen fibrils coated with mineral platelets prior to NaF treatment ((A) and (B)). After 1 s of NaF treatment ((C) and (D)) the underlying collagen fibril banding starts to appear (arrow, (D)). After 10 s of NaF treatment ((E) and (F)), the collagen fibril surface becomes almost completely exposed. However, a few individual platelets still remain attached to the collagen fibrils (arrows, (F)).

cut and freed of marrow as described above. The samples were dried in a desiccator at 37 °C for 2 h and then weighed on a precision scale (AJ100, Mettler Toledo Ltd, Switzerland). Three of the samples were then placed in a 0.5 M EDTA solution buffered with 10 mM Hepes, 150 mM NaCl buffer at pH 8.0. The other three were placed in a saturated solution of NaF buffered with 10 mM Hepes, 150 mM NaCl buffer at pH 7.0. After 18 h, the samples were briefly rinsed in H_2O, dried in a desiccator and weighed again. The resulting samples were then placed in fresh solutions of either EDTA or NaF. This treatment process was repeated after 42 and 71 h, respectively. The significance of the difference in mass between the samples treated with EDTA and NaF was investigated using the two-tailed Student's *t*-test (StatView, Abacus Concepts, Berkeley, CA, USA). This test was done with a significance level p equal to 0.0001.

2.6. Gel electrophoresis—SDS PAGE

Pieces of trabecular bone from bovine vertebrae were cut into 2–3 mm thick sections and cleaned with a jet of ultra-pure water to remove the marrow and other particulates. The resulting samples were rinsed with ultra-pure water and lyophilized until dry. The material was then ground with a mortar and pestle under liquid nitrogen to a fine powder. Approximately 90 mg of the powdered sample was suspended in tris-glycine SDS sample buffer (Invitrogen, Carlsbad, CA, USA) and reduced with DTT. Additional solutions of 1.5 M NaF or NaCl were added to bring the final fluoride or chloride concentrations in each sample to 0.6 M (total sample volume of 180 μl), i.e. ~0.6 times the concentration of the saturated solution. Following sonication for 30 min, and heat denaturation at 85 °C for 20 min, the suspensions were centrifuged for 30 min at 14 000 rpm. 20 μl of the supernatant from each condition (NaF or NaCl treated) was loaded in duplicate on a 4–20% NOVEX tris-glycine SDS PAGE gel (Invitrogen) and run for 2 h at 125 V. For staining, each half of the gel (each containing one NaCl and one NaF treated sample) was stained with either NOVEX Colloidal Blue (Coomassie) stain (Invitrogen) or GelCode Glycoprotein stain (Pierce Biotechnology, Rockford, IL, USA). Following staining, the two gel halves were realigned and photographed side by side so that a direct comparison of the different staining results could be made.

3. Results

The initial AFM images of dried fracture surfaces (performed on six samples for each treatment) of bovine bone were recorded in dry N_2 gas. Figure 1 shows images of samples before (figures 1(A) and (B)) and after treatment with H_2O (figures 1(C) and (D)) and EDTA (figures 1(E) and (F)), and figure 2 shows images of samples before (figures 2(A) and (B)) and after (figures 2(C) to (F)) treatment with NaF. All samples exhibited similar morphologies, consisting of mineralized collagen fibrils measuring ~100 nm diameter, with average particle sizes of (33 ± 12) nm in width and (47 ± 18) nm in length and an average aspect ratio of 1.4 ± 0.3, consistent with results obtained from previous studies using other imaging techniques [1, 3, 11, 14, 22, 36, 37] (figures 1(A), (B), 2(A) and (B)). AFM images were also

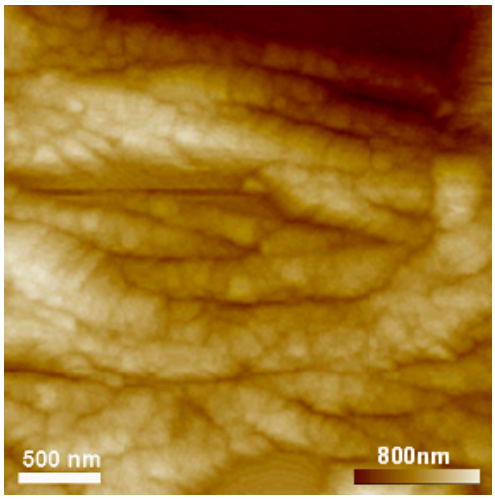

Figure 3. AFM height image of a fracture surface of human trabecular bone, imaged in NaCl buffer, showing similar collagen fibrils, densely coated with mineral platelets, as in figures 1 and 2.

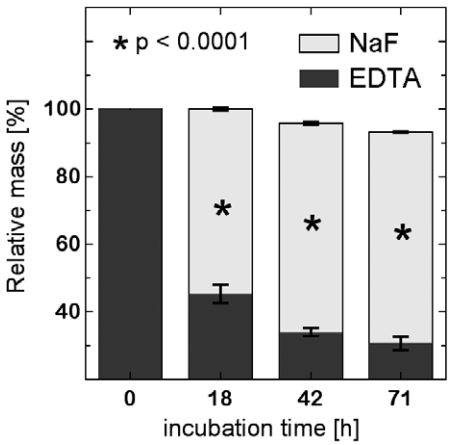

Figure 4. Average dry mass versus treatment time of three samples, each either incubated with NaF or EDTA in a Na-buffer. While the EDTA treatment decreases the dry mass by up to 69%, which is the expected mineral content, the NaF treatment decreases the dry mass by only 7%. Error bars indicate standard deviations and the asterisk indicates a significant difference ($p < 0.0001$) of dry mass between NaF and EDTA treated samples.

acquired from similar fracture surfaces of human bone in buffer solutions (150 mM NaCl, 10 mM Hepes, pH 7.0), as shown in figure 3. The morphology of samples imaged in buffer solution (figure 3) and samples imaged in dry N_2 (figures 1 and 2) appeared to be similar; mineralized collagen fibrils were characteristically encountered on all fractured surfaces investigated here. It is noteworthy that typically a slightly lower image resolution is achieved, if such rough topographies are imaged. The resolution is further lowered through imaging in an aqueous environment. The streaks, visible in the left corner of figure 2(A) and in figure 3 are caused by tip–surface convolution, artefacts, routinely observed on steeped profiled topographies, and whose impact depends on the tip aspect ratio.

As a control experiment, the solubility of the mineralized collagen fibrils (figures 1(A) and (B)) in water was investigated. For these experiments, all samples were exposed for approximately 2 min to HPLC grade water and subsequently dried under streaming N_2. The same location was then imaged again. In all cases, no significant morphological changes on a z scale of ∼1 nm were observed (cf. figures 1(A)–(D)). In contrast, a high-pressure water jet can mechanically alter the surface morphology and remove the mineral platelets [31, 38].

Chemical treatment with a 30 mM EDTA solution at pH 8, for about 20 s, and rinsing in a steady flow of HPLC grade water for 2 min completely changed the morphology of fracture surfaces. Following treatment, bare collagen fibril networks, characterized by their typical D-banding (with 67 nm periodicity), were clearly resolved (figures 1(E) and (F)). Similar morphological changes were observed when the freshly prepared bovine samples were exposed to a saturated aqueous solution of NaF (pH 7.0), clearly revealing the characteristic 67 nm banding pattern of the underlying collagen fibrils. In contrast to the EDTA-treated samples, the images obtained from those treated with NaF revealed the presence of a few remaining mineral platelets present on fracture surfaces. These platelets exhibited similar sizes and shapes as those seen during initial imaging of the untreated fracture surface (cf. figure 2(A)). A few round protrusions, possibly mineral particles, remained even after 10 s of exposure to NaF (white arrows in figure 2(F)).

Both treatments, EDTA and NaF, dramatically altered (in a nearly indistinguishable manner from one another) the fracture surface morphology. However, significant differences between these two chemical treatments were observed for bulk samples, as described below.

Cuboid bovine trabecular bone samples, (5 mm × 5 mm × 4 mm in size) devoid of bone marrow were incubated in either saturated NaF or 0.5 M EDTA solutions. Their dry mass was measured prior to and at 18, 42 and 71 h intervals during the course of incubation.

While the EDTA-treated samples lost 55% of their dry mass during the first 18 h, there was no detectable relative dry mass loss in the NaF-treated samples after the same time period, as shown in figure 4. After 71 h, the EDTA-treated samples lost ∼69% of their dry weight while the NaF-treated samples only decreased in weight by ∼7%. The weight of the EDTA-treated bone samples (∼31% of their initial dry mass) after three days' exposure, is within the range of the dry mass percentage of their organic constituents (30–35%) [39].

To investigate whether NaF treatment also influences protein extractability, we performed SDS-PAGE on lyophilized trabecular bovine bone powder in the presence of either 0.6 M NaCl or 0.6 M NaF. In the latter case, significantly greater extractable protein yield was obtained as seen in figure 5. We also observed that the protein extraction in the presence of NaF yielded a comparatively higher percentage of glycoproteins as well as a specific band at ∼66 kDa.

4. Discussion

The AFM images of bovine trabecular bone fracture surfaces presented here reveal, for the first time, time-lapsed *in*

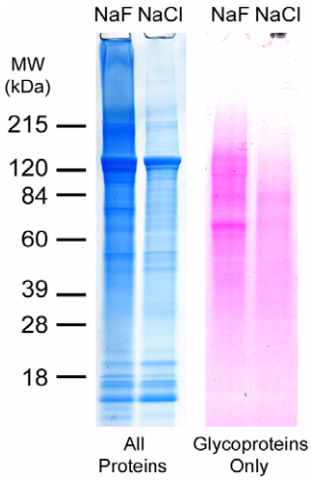

Figure 5. SDS-PAGE of protein extracted from bovine trabecular bone in the presence of NaF and NaCl, stained with NOVEX Colloidal Blue (Coomassie) stain or Gelcode Glycoprotein stain. Significantly more protein is extracted in the presence of NaF and staining for glycoproteins shows that a distinct band appears at about 66 kDa when the extraction is done in the presence of NaF, further supporting the evidence that NaF weakens organic binding within bone composite interfaces.

situ imaging of trabecular bone with nanometre spatial resolution during different chemical treatments. The images of fracture surfaces are in agreement with the previous AFM investigations of Sasaki *et al* [40] but provide significantly higher spatial resolution. In our study, different imaging conditions—imaging in solution for human bone, rapid buffer removal and subsequent dry imaging for bovine bone—yield comparable results. This suggests that the observed features are meaningful, and not caused by drying artefacts, e.g. from buffer salt residues (cf. figures 1–3). Since imaging in liquid yielded similar results, but in our case somewhat lower spatial resolution, we investigated the effect of EDTA and NaF treatments on fracture surfaces of trabecular bone dried after each respective treatment. Generally, we discovered mineralized collagen fibrils, on fracture surfaces, suggesting that bone fails within the interfibrillar interface, which is in agreement with previously published results [14, 22, 31, 37].

The fact that the hydroxyapatite platelets are removed following EDTA treatment at low concentrations, but not significantly altered by water treatment, as shown in figure 1, reveals that EDTA is, in fact, responsible for mineral platelet dissolution, the results of which are consistent with the data obtained from the mass loss experiments shown in figure 4. Surprisingly, fracture surfaces treated with NaF showed similar morphological features as those treated with the mineral dissolving solution of EDTA; removal of the mineral platelets resulted in the exposure of the underlying collagen fibrils as seen in figures 1 and 2. On the other hand, the time-lapsed mass loss observation presented in figure 4 clearly shows that treatment with the highly concentrated solutions of NaF exhibited a significantly lower mineral dissolution potential, as also reported previously [41]. It should be noted here that the fracture surfaces changed their morphology after only seconds of treatment while the bulk mass loss occurred over many hours. This can be understood when one considers that the necessary penetration depth of the agent (NaF or EDTA) is between zero and a few nm for the surface treatment, and on the order of a few 100 μm (typical trabecular thickness) for the bulk samples.

Fluoride ions are known to substitute with the hydroxide ions of apatite crystals. Theoretical and experimental results suggest that this substitution occurs superficially, eventually resulting in precipitation of CaF_2, which is then layered on the hydroxyapatite surface [42]. The NaF treatment also appears to significantly weaken the organic/mineral interfaces of bone, otherwise it would be difficult to explain the apparently rapid removal of mineral platelets by using a chemical treatment method that is known to not significantly alter hydroxyapatite solubility. Furthermore, a few remaining protrusions, possibly mineral particles, can be seen on the NaF-treated surface. If confirmed, this would be further evidence that the collagen fibril was exposed following particle detachment, rather than particle dissolution.

The crystal surfaces of the carbonated hydroxyapatite in bone are expected to be calcified and these surfaces are bridged with the negatively charged polyelectrolytes, i.e. (NCPs), attached to the organic backbone (collagen type I) [43–45]. Hydrogen-bonding networks and NCPs are thought to cooperatively stabilize this interface [46]. The fluorination of the calcified interface is expected to induce precipitation and formation of superficial CaF_2, thus leading to the subsequent disordering of this highly complex interface. This NaF-induced formation and precipitation of CaF_2 was previously observed on bioapatite [47, 48].

The nature of the interfacial structure between the main organic and inorganic components of bone, i.e. collagen fibrils and hydroxyapatite, is still a matter of ongoing debate. In any case, the treatment with highly concentrated solutions of NaF results in the apparent failure of the organic–mineral interface, and ultimately in mineral platelet detachment from the underlying collagen fibrils.

The coincident removal of particles from collagen fibrils following NaF treatment coupled with the more efficient extraction of a range of unidentified glycoproteins suggests that these extracted proteins were previously attached to hydroxyapatite and thus potentially part of the organic–inorganic interface. NCPs are known to control bone mineralization, and their presence at locations between mineralized collagen fibrils was reported previously [49]. Thus, one can speculate that these proteins might also function as linkers, attaching extrafibrillar mineral to the collagen fibrils' exterior, and mineralized collagen fibrils to each other. Such speculation is backed by the recent finding that bone sialoprotein (BSP), one of the most abundant NCPs in bone, binds to collagen type I [50]. In addition, NCP extraction experiments have shown distinct groups of collagen-bound and mineral-bound bone proteins [13, 51]. Raif and Harmand categorized these NCPs as either mineral-bound or organic-bound and further suggested that the mineral–collagen link is formed by a complex NCP network [51]. The results reported here, however, cannot help resolve such speculation and further research is required to determine exactly which proteins in bone are involved in such binding or linking processes. Nevertheless, our results nicely complement prior work investigating mainly the effects of NaF treatment on bone

biomechanics; NaF treatment was previously found to decrease bone strength *in vivo* [52], as well as *in vitro* [15, 24–26] without significantly affecting bone mineral density [23]. From such experiments it was concluded that NaF weakens the organic–inorganic interface in bone for which we present, for the first time, a direct visual proof.

5. Conclusion

In this paper we demonstrate the unique capabilities of AFM for investigating the ultrastructure of tissue surfaces with similar spatial resolution as is achieved by transmission electron microscopy (TEM). The fact that the AFM is capable of imaging the topography of surfaces created during a fracture event complements the wealth of information that can be retrieved from state-of-the-art TEM and scanning electron microscopy studies. Our results provide a visual proof for the hypothesis that NaF treatment of bone detrimentally alters the hydroxyapatite–collagen interface, resulting in mineral platelet detachment, revealing (as in the case of the EDTA-treated samples) the pristine collagen fibrils exhibiting a typical corrugation with 67 nm in length. In addition, NaF was found to be a potent agent for gently extracting proteins from ground bone powder.

Acknowledgments

This work was supported by the National Science Foundation through the UCSB Materials Research Laboratory under Award DMR00-80034, by the National Institutes of Health under Award GM065354, by the NASA University Research, Engineering and Technology Institute on Bio-inspired Materials under Award No. NCC-1-02037, and by a research agreement with Veeco Inc. No. SB030071. PJT acknowledges SNF postdoctoral fellowship No. PA002—111445, MEL acknowledges DFG postdoctoral fellowship No. 1981-1, GS acknowledges SNF postdoctoral fellowship No. PA002-108933 and GEF acknowledges an ÖAW DOC Fellowship. Human tissue samples used in this work were supplied by the National Disease Research Interchange (NDRI).

References

[1] Weiner S and Wagner H D 1998 *Annu. Rev. Mater. Sci.* **28** 271–98
[2] Weiner S, Traub W and Wagner H D 1999 *J. Struct. Biol.* **126** 241–55
[3] Rho J Y, Kuhn-Spearing L and Zioupos P 1998 *Med. Eng. Phys.* **20** 92–102
[4] Fratzl P, Gupta H S, Paschalis E P and Roschger P 2004 *J. Mater. Chem.* **14** 2115–23
[5] Keckes J, Burgert I, Fruhmann K, Muller M, Kolln K, Hamilton M, Burghammer M, Roth S V, Stanzl-Tschegg S and Fratzl P 2003 *Nat. Mater.* **2** 810–4
[6] Mayer G and Sarikaya M 2002 *Exp. Mech.* **42** 395–403
[7] Aizenberg J, Weaver J C, Thanawala M S, Sundar V C, Morse D E and Fratzl P 2005 *Science* **309** 275–8
[8] Weaver J C *et al* 2007 *J. Struct. Biol.* at press (doi:10.1016/j.jsb.2006.10.027)
[9] Gao H, Ji B, Jager I L, Arzt E and Fratzl P 2003 *Proc. Natl Acad. Sci. USA* **100** 5597–600
[10] Prockop D J and Fertala A 1998 *J. Struct. Biol.* **122** 111–8
[11] Weiner S and Traub W 1992 *Faseb J.* **6** 879–85
[12] Kindt J H, Fantner G E, Thurner P J, Schitter G and Hansma P K 2005 *Mater. Res. Soc. Symp. Proc.* **874** L5.12.1–7
[13] Grynpas M D, Tupy J H and Sodek J 1994 *Bone* **15** 505–13
[14] Fantner G E *et al* 2005 *Nat. Mater.* **4** 612–6
[15] Walsh W R and Guzelsu N 1994 *Biomaterials* **15** 137–45
[16] Walsh W R, Ohno M and Guzelsu N 1994 *J. Mater. Sci. Mater. Med.* **5** 72–9
[17] Smith B L, Schaffer T E, Viani M, Thompson J B, Frederick N A, Kindt J, Belcher A, Stucky G D, Morse D E and Hansma P K 1999 *Nature* **399** 761–3
[18] Gupta H S, Wagermaier W, Zickler G A, Aroush D R B, Funari S S, Roschger P, Wagner H D and Fratzl P 2005 *Nano Lett.* **5** 2108–11
[19] Braidotti P, Branca F P and Stagni L 1997 *J. Biomech.* **30** 155–62
[20] Thurner P J, Wyss P, Voide R, Stauber M, Stampanoni M, Sennhauser U and Muller R 2006 *Bone* **39** 289–99
[21] Braidotti P, Bemporad E, D'Alessio T, Sciuto S A and Stagni L 2000 *J. Biomech.* **33** 1153–7
[22] Thurner P J, Erickson B, Jungmann R, Schriock Z, Weaver J C, Fantner G E, Schitter G, Morse D E and Hansma P K 2007 *Eng. Fract. Mech.* at press (doi:10.1016/j.engfracmech.2006.05.024)
[23] DePaula C A, Abjornson C, Pan Y, Kotha S P, Koike K and Guzelsu N 2002 *J. Biomech.* **35** 355–61
[24] Kotha S P, Walsh W R, Pan Y and Guzelsu N 1998 *Bio-Med. Mater. Eng.* **8** 321–34
[25] Silva M J and Ulrich S R 2000 *J. Biomech.* **33** 231–4
[26] Walsh W R, Labrador D P, Kim H D and Guzelsu N 1994 *Ann. Biomed. Eng.* **22** 404–15
[27] Bird D M, Carriere D and Lacombe D 1992 *Arch. Environ. Contamin. Toxicol.* **22** 242–6
[28] Wolinsky I, Simkin A and Guggenheim K 1972 *Am. J. Physiol.* **223** 46–50
[29] Fratzl P, Schreiber S, Roschger P, Lafage M H, Rodan G and Klaushofer K 1996 *J. Bone Miner. Res.* **11** 248–53
[30] Chachra D, Turner C H, Dunipace A J and Grynpas M D 1999 *Calcif. Tissue Int.* **64** 345–51
[31] Hassenkam T, Fantner G E, Cutroni J A, Weaver J C, Morse D E and Hansma P K 2004 *Bone* **35** 4–10
[32] Habelitz S, Balooch M, Marshall S J, Balooch G and Marshall G W Jr 2002 *J. Struct. Biol.* **138** 227–36
[33] Danielsen C C, Andreassen T T and Mosekilde L 1986 *Calcif. Tissue Int.* **39** 69–73
[34] Marti O, Drake B and Hansma P K 1987 *Appl. Phys. Lett.* **51** 484–6
[35] Kindt J H, Sitko J C, Pietrasanta L I, Oroudjev E, Becker N, Viani M B and Hansma H G 2002 *At. Force Microsc. Cell Biol.* **68** 213–29
[36] Landis W J, Hodgens K J, Arena J, Song M J and McEwen B F 1996 *Microsci. Res. Technol.* **33** 192–202
[37] Fantner G E *et al* 2006 *Compos. Sci. Technol.* **66** 1202–8
[38] Hassenkam T 2005 private communication
[39] Turek S L and Lippincott J B 1985 *Orthopaedics: Principles and Applications* 2nd edn, p 113 and 136
[40] Sasaki N, Tagami A, Goto T, Taniguchi M, Nakata M and Hikichi K 2002 *J. Mater. Sci. Mater. Med.* **13** 333–7
[41] Dorozhkin S V 2002 *Progr. Cryst. Growth Charact. Mater.* **44** 45–61
[42] de Leeuw N H 2004 *Phys. Chem. Chem. Phys.* **6** 1860–6
[43] Bradt J H, Mertig M, Teresiak A and Pompe W 1999 *Chem. Mater.* **11** 2694–701
[44] Song J, Malathong V and Bertozzi C R 2005 *J. Am. Chem. Soc.* **127** 3366–72
[45] Girija E K, Yokogawa Y and Nagata F 2004 *J. Mater. Sci. Mater. Med.* **15** 593–9
[46] Wilson E E, Awonusi A, Morris M D, Kohn D H, Tecklenburg M M J and Beck L W 2006 *Biophys. J.* **90** 3722–31

[47] Wen H B, Cui F Z, Chen X Q, Wang Q and Li H D 1995 *Caries Res.* **29** 122–9
[48] Freeman J J, Wopenka B, Silva M J and Pasteris J D 2001 *Calcif. Tissue Int.* **68** 156–62
[49] McKee M D and Nanci A 1996 *Microsc. Res. Technol.* **33** 141–64
[50] Tye C E, Hunter G K and Goldberg H A 2005 *J. Biol. Chem.* **280** 13487–92
[51] Raif E M and Harmand M F 1993 *Biomaterials* **14** 978–84
[52] Turner C H, Hasegawa K, Zhang W, Wilson M, Li Y and Dunipace A J 1995 *J. Dent. Res.* **74** 1475–81